Hindawi
Journal of Nanomaterials
Volume 2018, Article ID 5953609, 13 pages
https://doi.org/10.1155/2018/5953609

Review Article

A Brief Overview of TiO_2 Photocatalyst for Organic Dye Remediation: Case Study of Reaction Mechanisms Involved in Ce-TiO_2 Photocatalysts System

Milind Pawar,[1] **S. Topcu Sendoğdular**,[2,3] **and Perena Gouma**[1,2]

[1]*MSE Department, Ohio State University, Columbus, OH 43210, USA*
[2]*MSE Department, SUNY Stony Brook, Stony Brook, NY 11794, USA*
[3]*MSE Department, Erciyes University, Talas, Kayseri, Turkey 38039*

Correspondence should be addressed to Milind Pawar; pawar.38@osu.edu

Received 30 April 2018; Revised 10 August 2018; Accepted 14 August 2018; Published 8 October 2018

Academic Editor: P. Davide Cozzoli

The ever-increasing world population and the rapid growth of industrialization globally make necessary the development of clean technologies and affordable materials for remediating environmental pollution from petroleum-based hydrocarbons and dyes, among others. Advanced photocatalytic materials may provide an excellent solution for environmental cleanup without generating toxic byproducts as they allow for the complete oxidation of the pollutants and their conversion to benign species. In this review, the basic principle of photocatalyst operation and the importance of bandgap engineering are discussed. TiO_2 has been the default photocatalyst although it has several shortcomings. Doping of TiO_2 with Ce has been explored extensively in the literature as a way to enable visible-light-activated photocatalysis and enhanced efficiency. Recent advances in the synthesis of Ce-modified TiO_2 photocatalytic materials along with photocatalytic reaction mechanisms are summarized.

1. Introduction

The sun is radiating clean energy without any pollutants from billions of years, and it is the most crucial source of energy for life on our planet earth. Amount of solar energy reach on the earth's surface in a single day can satisfy the energy requirement of mankind for a decade. It is of utmost importance to utilize the abundance of solar energy for a variety of applications such as energy production and environmental cleanup. Wastewater recycling via photocatalyst may pose a solution to the long-standing shortage of fresh water in many countries. A photocatalyst is a material that helps to accelerate and enhance a light-induced reaction without being consumed in the process [1]. Recently, there has been significant interest in the development of novel photocatalytic technology covering an extensive range of environmental applications such as water remediation and environmental cleanup of oil spills and other pollutants. There have also been some energy-related studies, which focus on the use of photocatalysts for fuel production (e.g., H_2), specifically through water splitting. Environmental cleanup by using photocatalysts offers many benefits [2]: conversion of pollutants from complex molecules into simple and nontoxic substances and avoidance of secondary treatment, disposal, or use of any expensive oxidizing chemicals by utilization of solar energy. Numerous studies were published on the photocatalytic applications of titania (TiO_2) for the decomposition of organic compounds due to the ability of TiO_2 to oxidize organic and inorganic substances in water and air through redox processes [3–5]. TiO_2 only absorbs ultraviolet (UV) light of broad solar spectrum due to its large bandgap energy ($\lambda < 388$ nm), which was comprised of only 3% of the entire solar spectrum. In order to overcome this issue, cerium- (Ce-) doped TiO_2 photocatalysts are explored extensively for utilization of visible light to activate TiO_2 photocatalyst. This review is focused on Ce-doped TiO_2 photocatalysts for advanced oxidation process (AOP) of degradation of organic dyes. Complex

Table 1: Bandgap energies of semiconductors as photocatalyst.

Photocatalyst	Bandgap energy (eV)
ZrO_2	5.0
ZnS	3.6
TiO_2 (anatase)	3.2
TiO_2 (rutile)	3.0
WO_3	2.8
SnO_2	2.5
Fe_2O_3	2.3
GaP	2.25
V_2O_5	2.6
CuO	1.7
CdSe	1.7
MnO_2	0.25
CeO_2	2.94

reaction mechanisms involved in Ce-doped TiO_2 proposed by various researchers in the field are summarized to provide a comprehensive review.

1.1. Basic Principle of Oxide-Based Photocatalysts. An ideal photocatalyst should be activated by photons, chemically nonreactive, easily available, nontoxic, and able to utilize a broad solar spectrum [6]. Energy difference of valence band (VB) and conduction band (CB) is known as bandgap (E_g), which determines if the material is a conductor, a semiconductor, or an insulator. Unlike insulators or metals, semiconductors have the bandgap that allows producing electron (e^-)/hole (h^+) pairs when they absorb a photon with energy equals to their bandgap or higher than that. Semiconducting metal oxides are commonly used as photocatalysts due to their favorable bandgap (E_g) and band edge positions. In semiconductors, the electronic structure plays an important role where the valence band (VB) of the semiconductor is completely filled with electrons and the conduction band (CB) is empty. The bandgap of different semiconductor materials varies as per their electronic structure. Some of the semiconductor oxide materials bandgap is presented in Table 1.

The underlying mechanism of semiconductor photocatalysts (TiO_2, ZnO, ZnS, and Fe_2O_3) is shown in Figure 1. As shown in Figure 1, when a photon with adequate energy (≥bandgap energy of semiconductor) is absorbed by the semiconductor, an electron from valence band (VB) gets excited and jumps to the conduction band (CB), which generates a hole in the valence band. This process of electron-hole pair generation is known as photoexcitation. Photoexcited electrons can be utilized in the reduction of oxygen, and similarly, holes can be utilized in oxidizing water molecules which are adsorbed on photocatalyst surface.

Photoexcitation: $h\nu \geq E_g$, TiO_2 (photocatalyst) + $h\nu$ (photon) ➔ h^+_{VB} (hole in valence band) + e^-_{CB} (electron in conduction band).

Here, h: Planck's constant $6.62607004 \times 10^{-34}$ m^2 kg/s; v: frequency of incident light.

Following the photoexcitation process, as shown in Figure 2, several paths can be followed by the photogenerated electron and hole because of adsorbed species on the photocatalyst surface. Here, electron acceptor species can be reduced by electron (pathway [a]: $A + e^- \rightarrow A^-$); similarly, electron donor species can be oxidized by combining with the hole (pathway [b]: $D \rightarrow D^+ + e^-$). Recombination of electron and hole may occur on the surface of semiconductor particle (pathway [c]: $h^+ + e^- \rightarrow$ photocorrosion) or within the volume of the semiconductor particle (pathway [d]) [1]. The process of electron and hole recombination is known as photocorrosion, where electron and hole lose their redox ability by generating thermal energy or a photon.

Adsorbed water on photocatalyst surface splits into $^{\cdot}OH$ and H^+ when oxidized. These hydroxyl radicals can easily oxidize organic contaminants. Cationic radicals $^{\cdot}RH^+$ can be produced by direct oxidation of adsorbed organic pollutants (RH) with holes in VB. On the other side, the generation of superoxide radical anions ($^{\cdot}O_2^-$) occurs due to the reduction of oxygen by the electron. Hydrogen dioxide in conduction band can be produced by the reaction of radical anion and H^+. Reactive oxygen species (ROS) that result from chain reaction are as shown in Figure 3 [7].

1.2. The Bandgap Position. The redox potentials and the bandgap position of a photocatalyst are important factors controlling the photo-induced electron excitation. Semiconductors should allow for different redox reactions under light irradiation. The conduction band of photocatalyst should be at positive potential as compared to the acceptor's potential in order to transfer an electron to the acceptor. Similarly, the potential level of the valence band is required to be more negative than the donor in order to accept electron [8]. Figure 4 illustrates the valence and conduction band positions for various semiconductors. The bandgap energy determines which semiconductor material can be activated by the light of different wavelengths. TiO_2 has been extensively explored because of its photocatalytic activity under ultraviolet and visible light. TiO_2 has two primary phases: rutile and anatase. Anatase has higher bandgap with 3.2 eV, which is equivalent to an excitation wavelength of 388 nm, capable of absorbing light near the UV range. Rutile exhibits 3.0 eV with 410 nm wavelength, which absorbs visible light.

The factors affecting the efficiency of photocatalysis are as follows:

(i) Intensity of Light Source. The photocatalytic activity of semiconductor oxides depends on the intensity of light absorption. Better photocatalytic efficiency can be achieved with an increase in the intensity of light as it improves charge separation [9].

(ii) Nature of the Photocatalyst. Kogo et al. reported that photocatalytic reaction efficiency can be affected by the number of absorbed photons by photocatalysts surface [10]. It implies that photocatalytic reactions take place on the adsorbed surface. Surface morphologies such as particle size and shape are important factors affecting the function of nanomaterials' photocatalysis process [11]. Different synthesis methods have been developed to exhibit the necessary size, shape, and stability for their applications [12].

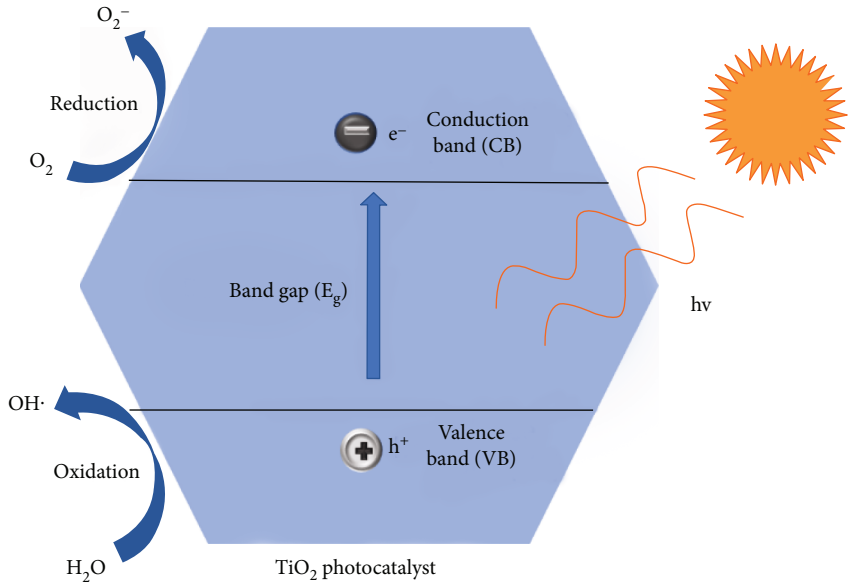

Figure 1: Basic mechanism of semiconductor photocatalyst.

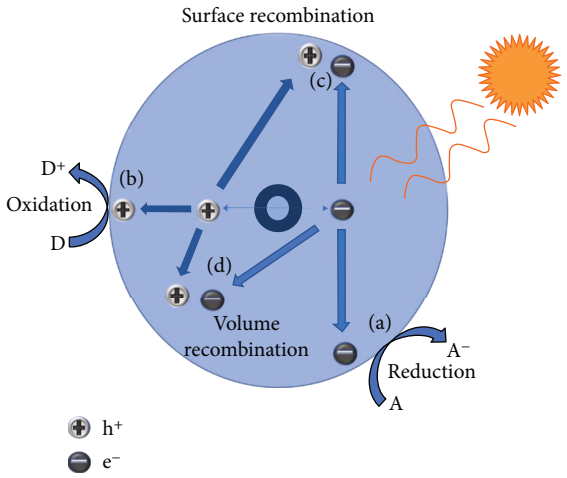

Figure 2: Schematic of charge separation and photogenerated hole and electron (adopted with permission from Linsebigler et al.) [8].

(iii) pH of the Solution. Surface charge properties can be governed by pH of solution and size of aggregates [13] due to the different charge of the semiconductor surface.

(iv) Temperature. When the temperature of the reaction raises, the photocatalytic efficiency decreases due to the enhanced recombination of e^-/h^+ pairs and enhanced desorption of adsorbed species from the exterior of the photocatalyst.

(v) Quantity of the Photocatalyst. It is considered that the photocatalytic activity can be increased with increasing the concentration of the catalyst [14]. However, the level of catalyst concentration has to be determined because the excess catalyst prevents the diffusion of the light into the solution which might result in unfavorable light scattering [15].

1.3. TiO_2 Photocatalyst. As a photocatalyst, titanium dioxide (TiO_2) has attracted substantial attention for a long time and is considered as one of the most promising materials for commercial use due to its outstanding optical and electronic properties, photoactivity, high chemical stability, low cost, nontoxicity, reusability, and eco-friendliness [8, 16, 4]. Much more attention has been focused on the different preparation methods of TiO_2 in order to improve its performance compared to commercial TiO_2 powders (for example, Degussa P25).

The crystallographic structure of TiO_2 is shown in Figure 5 [17]. Well-known phases of TiO_2 are anatase, rutile, and brookite. Rutile is a tetragonal ($a = 4.5937$ Å, $c = 2.9587$ Å), anatase is also a tetragonal ($a = 3.7845$ Å, $c = 9.5143$ Å), and brookite is an orthorhombic crystal ($a = 5.4558$ Å, $b = 9.1819$ Å, $c = 5.1429$ Å). C coordinate of anatase is higher than other phases, and c/a ratio of its unit cell is greater than rutile and brookite phases. Among all these phases, anatase is the most active allotropic phase regarding photocatalytic activity when compared to rutile, brookite, and TiO_2-B (artificial phase).

Rutile is thermodynamically stable at ambient conditions, whereas anatase is kinetically stable, and it transforms to rutile at higher temperatures [18] depending on the particle size, ambient pressure, and other parameters [19]. Brookite phase is also metastable but difficult to synthesize, hence it is seldom studied [20]. Table 2 represents the oxide polymorphs of TiO_2 with experimental condition and method for synthesis as well as particle size. Among the three different crystalline phases of TiO_2, anatase shows the highest stability for particle size less than 11 nm. Similarly, rutile shows thermodynamic stability for particle size greater than 35 nm, and for brookite, it is 11–35 nm which are summarized in Table 2 [21].

At room temperature, the rutile phase is thought to be a more stable phase as compared to the anatase in the case of

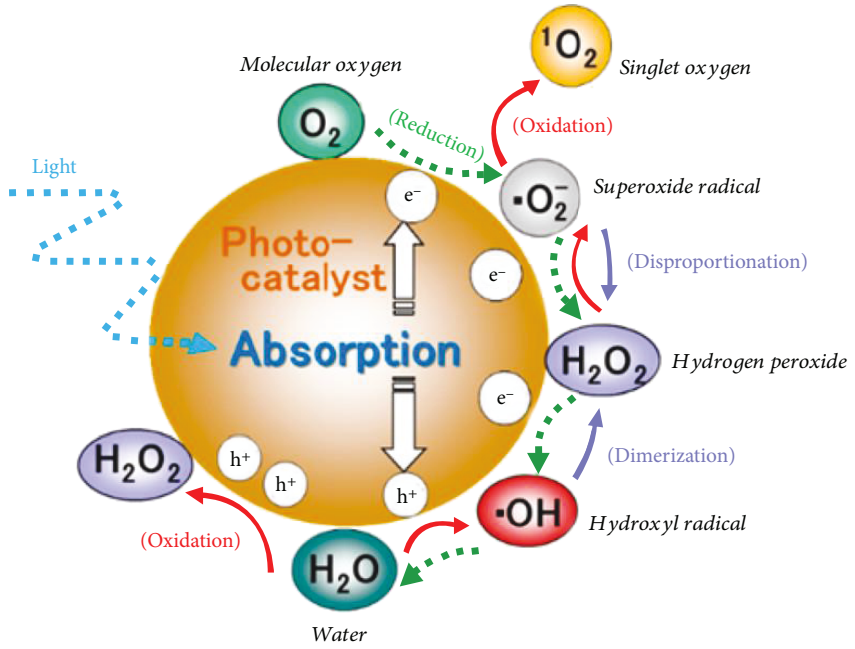

Figure 3: Production of reactive oxygen species by chain reaction (reprinted with permission from Nosaka and Nosaka) [7].

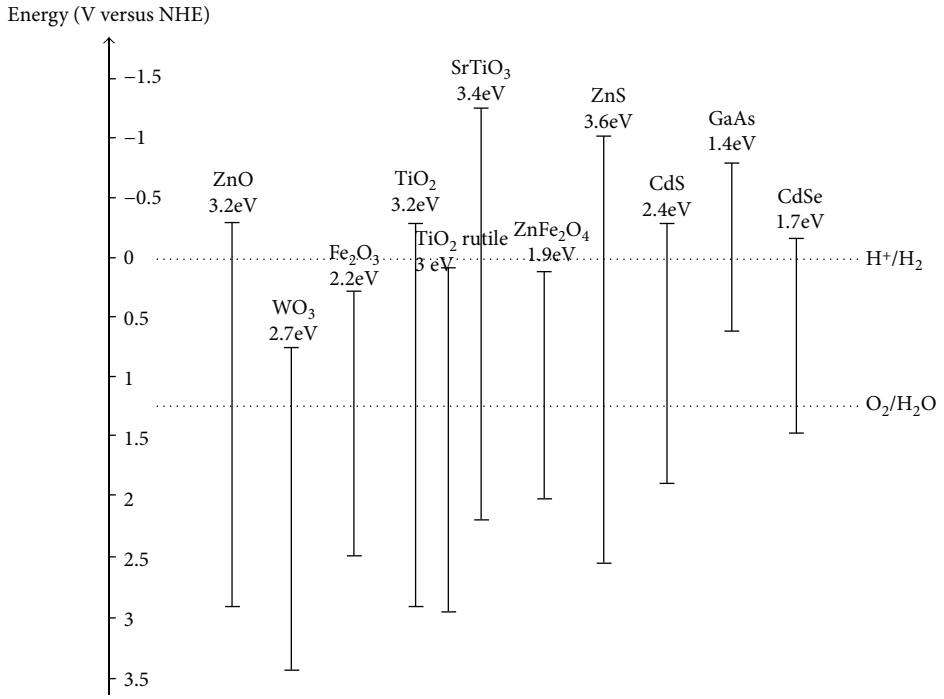

Figure 4: Band edge position with redox potentials for different semiconductors (adapted from Zhang et al.) [81].

bulk TiO_2. However, it was suggested by Zhang and Banfield and independently confirmed by Gouma that anatase becomes a more stable phase due to lower total free energy as compared to rutile if the particle size is smaller than 14 nm [21, 22]. Subsequently, some studies have claimed that rutile and anatase together have higher photocatalytic activity as compared to 100% anatase. For example, the commercial TiO_2, Degussa P25, is a mixture of anatase (~75%) and rutile (~25%) phases, and it is the most widely used photocatalyst for environmental applications [23].

Anatase can be synthesized at lower temperatures (40°C) to nanoscale size; it shows better photocatalytic properties because nanoscale size increases the number of pores and enhances solid-solid interactions. On the contrary, at higher

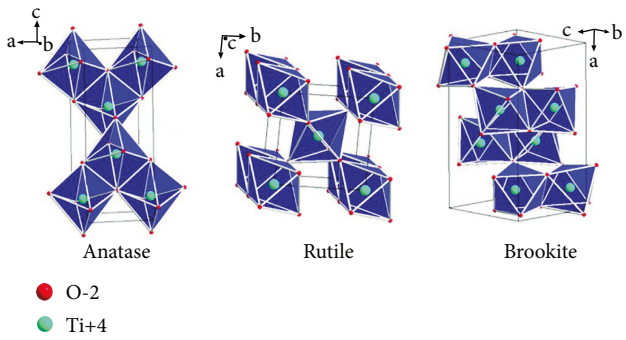

FIGURE 5: Common polymorphs of TiO_2 (reprinted with permission from Dambournet et al.) [17].

temperatures (above 300°C) nano-TiO_2 has worse photocatalytic activity [24]. The properties of brookite are poorly known because of the difficulties associated with synthesis of pure brookite phase. Tay et al. also shows that the synthesized two phases (anatase/brookite) have higher photocatalytic activity due to the electrons transfer from brookite conduction band (CB) to anatase CB resulting in efficient electron-hole separation [25].

1.4. Modified TiO_2. Two primary factors must be taken into account while designing the systems for conducting photocatalytic reactions. The first one is the efficiency of e^- and h^+ pair generation when the photocatalyst is illuminated with solar radiation. Second is the efficiency of the e^-/h^+ pair separation before they lose their redox ability due to recombination. The photocatalytic efficiency can be enhanced significantly by addressing the following primary issues: (i) increase the time of charge separation and recombination, (ii) broaden the solar spectrum range for photocatalyst, and (iii) changing the yield of a particular product [1, 8].

Semiconductor photocatalysis system can be designed by considering the stability of the material under the light, product selectivity, and activation wavelength range [8]. TiO_2 has been the most widely studied photocatalyst for many years. However, the main barriers of the TiO_2 are its activation by ultraviolet light ($\lambda \leq 400$ nm) because of the wide bandgap of TiO_2 (~3.2 eV for anatase and ~3.0 eV for rutile), for which it only absorbs UV light (only about 3% of overall solar spectrum) [26]. Another major drawback of TiO_2 is photogenerated electron-hole recombination, which deteriorates the photocatalytic activity [27]. Therefore, an apparent goal is the reducing bandgap of TiO_2 in order to shift the absorption band to the visible region and to enhance the electron-hole separation process. The modifications of TiO_2 have been accomplished by different strategies such as doping, codoping, sensitization, and coupling [28–32]. The coupling of two semiconductors provides different energy levels, which give a chance to improve a more efficient charge separation to enhance the lifetime of charge carriers and to increase interfacial charge transfer [33].

Rare-earth elements are ideal dopants because of their 4f electronic configuration and spectroscopic properties [34]. Modification of electronic structure as well as crystal structure of TiO_2 can be performed by doping rare-earth elements. Lanthanide ions could act as effective electron scavengers to trap the CB electrons from TiO2. Xu et al. [35] studied doping with rare-earth ions including La^{3+}, Ce^{3+}, Er^{3+}, Pr^{3+}, Gd^{3+}, Nd^{3+}, and Sm^{3+} in TiO_2 which improved photocatalytic activity in the degradation of nitrite. Wang et al. [36, 37] also illustrated doping with lanthanide ions (La^{3+}, Er^{3+}, Pr^{3+}, Nd^{3+}, and Sm^{3+}), which improved the photoelectrochemical properties as well as increased the photocurrent response and the photon current conversion efficiency in the range of 300–400 nm.

1.5. Cerium-Modified TiO_2 Photocatalyst. Cerium is one of the most reactive rare-earth metals and can be utilized in a broad range of applications in the field of catalysis and photocatalysis. It is also one of the most generous rare-earth elements, making up about 0.0046% of the Earth's crust by weight (64 ppm), even more abundant than copper (60 ppm) [38]. Cerium has Ce^{3+}/Ce^{4+} redox couple, which can shift between CeO_2 and Ce_2O_3 under reducing and oxidizing conditions [39, 40]. Furthermore, different electronic structures between Ce^{3+} ($4f^15d^0$) and Ce^{4+} ($4f^05d^0$) electronic configuration would lead to changed optical as well as catalytic properties [41]. The ability of Ce^{3+} to oxidize to Ce^{4+} states leads to high oxygen mobility that could result in strong catalytic potential [42], and because of this reason, it commonly applied in heterogeneous catalysis. However, CeO_2 does not show good thermostable behavior because of its rapid sintering under influence of elevated temperatures [43, 44].

Cerium oxide (ceria), CeO_2 has the face-centered cubic (fcc) fluorite structure with eight coordinate cations (oxygen atoms) and four coordinate anions (Figure 6). The complete unit cell, Ce_4O_8, measures 0.51 nm (5.1 Å) on edge [44]. Ceria being an n-type semiconductor has a bandgap of 2.94 eV. The favorable bandgap of ceria makes it active under UV-Vis range and its utilization as a photocatalyst in advanced oxidation processes.

Ceria is used in numerous catalytic reactions such as photocatalytic reactions and water splitting reactions, to name a few [45]. Recently, ceria has been explored as a dopant in aqueous phase photocatalytic reactions [36, 46].

The photocatalytic activity of Ce-TiO_2 for degradation of 2-mercaptobenzothiazole was reported by Li et al. [39]. The activity of Ce-TiO_2 was higher in comparison with pure TiO_2, and this was attributed to the higher surface area and better charge separation of photocatalyst [39]. Optical absorption was shifted to visible range 400–500 nm because of the introduction of Ce 4f level. Formation of 4f level and defect level were considered as a reason for delayed electron-hole recombination and activation of photocatalyst under UV visible light range [39].

The phase transformation of anatase to rutile was hindered by Ce ions for low concentrations [47, 48]. Liu et al. produced Ce-TiO_2 (3–7 wt % Ce) with sol-gel process and finally calcined at a different temperature. With increasing temperature, anatase phase showed growth for lower temperature domain for both pure TiO_2 and Ce-TiO_2 systems; however, when the temperature was increased from 600°C to 800°C, the transformation of anatase to rutile phase

Table 2: Particle size effect on phase stability of TiO_2.

	Phase	Conditions	Particle size (nm)	Techniques	References
TiO_2	Brookite	—	11 to 35	Sol-gel	[21, 73]
	Anatase	Room temperature	Below 11	Sol-gel	[21, 73]
	Rutile	Above 850°C	Higher than 35	Sol-gel	[21, 73]

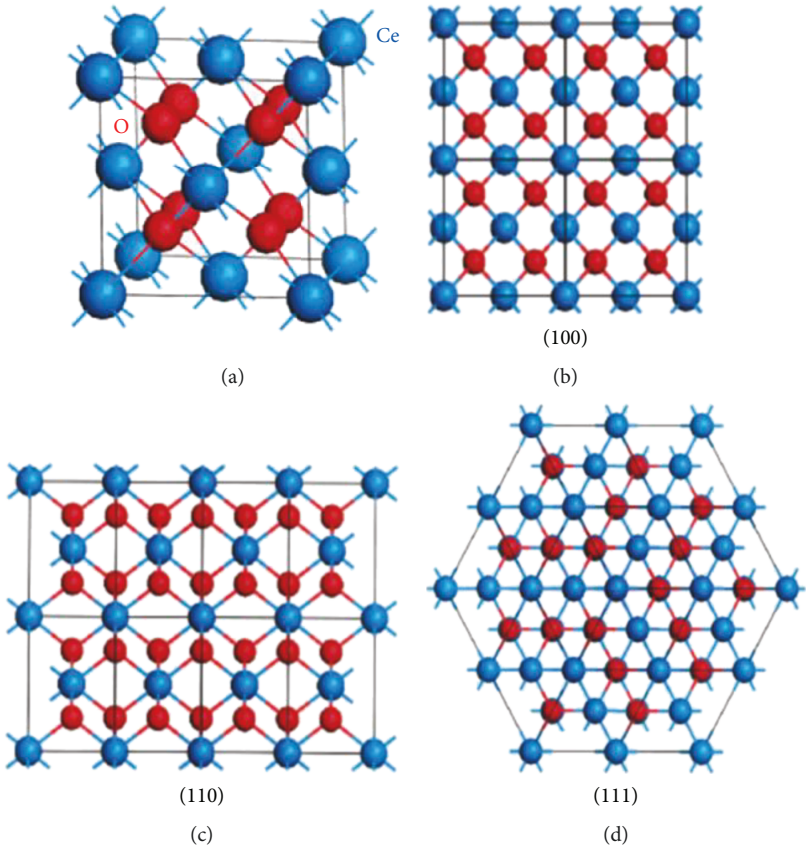

Figure 6: (a) Unit cell of the CeO_2 crystal structure; (b–d) (100), (110), and (111) planes of CeO_2 structure (reprinted with permission from Wang and Feng) [82].

was inhibited in the Ce–TiO_2 oxide. The main importance of this study was to show the shifting of light absorbance to the range of 380–460 nm in Ce–TiO_2 [48]. For higher amount of Ce, phase segregation of ceria on the surface of TiO_2 and rutile was formed [49].

López et al. represented the structure and morphology of the CeO_2–TiO_2 oxides that were prepared by the sol-gel method as 10 wt % and 90 wt % and then calcined at 473, 673, 873, and 1073 K temperatures [50]. Experimental results showed that better thermal stability for TiO_2 can be achieved by doping Ce ions to prevent particle sintering and subsequent pore collapsing [50]. Positive impact on crystallographic characteristic as well as sintering of photocatalyst was achieved by Ce doping. Distribution of cerianite on TiO_2 caused substitution of Ti^{4+} by Ce^{4+} within the TiO_2 anatase structure [50].

Cao et al. [51] synthesized 0.2% Ce-TiO_2 by the sol-gel method. The photodegradation test of methylene blue (MB) was carried out to assess the photocatalytic activity of Ce-TiO_2. Interesting behavior of first rising and then falling the degradation efficiency with an increase of Ce content was found. At low Ce content in the Ce-TiO_2, it is very easy for Ce^{4+} to capture the photogenerated electron and be reduced to Ce^{3+}, which in turn separates the electrons and holes effectively and subsequently improve the photocatalytic activity of TiO_2. However, when the Ce content exceeds a certain amount, the TiO_2 crystal lattice reduces the crystallinity because of high impurities and defects. This causes shortening of the trapping center distance, increases the chance of recombination of the photogenerated charge carriers in the trapping center, and thus reduces the photocatalytic efficiency in return.

Reli et al. [52] prepared novel cerium-doped TiO_2 with sol-gel method within surfactant Triton X-114 in cyclohexane and showed that 1.2 wt % Ce gives the maximum photocatalytic activity for the decomposition of ammonia under UV light radiation. Hierarchical CeO_2/TiO_2 nanofibrous mats were prepared by Cao et al. [53] via electrospinning

method. Photocatalysts prepared by electrospinning technique showed better photocatalytic efficiency for CeO_2/TiO_2 nanocomposite as compared to TiO_2 for the degradation of RB dye under UV light irradiation.

Eskandarloo et al. [54] represented TiO_2/CeO_2 hybrid photocatalysts, which were prepared from a powder mixture of titania and ceria. It was found that mixing TiO_2 with CeO_2 could facilitate efficient charge transfer, which can ease the separation of the photogenerated charge and in return increase photocatalytic efficiency [54]. Apart from here mentioned synthesis methods for Ce-TiO_2 photocatalyst, their morphology and particle size are summarized in Table 3.

1.6. Photocatalytic Degradation Mechanism of Ce-TiO_2 System. Various photocatalytic reaction mechanisms have been proposed so far depending upon the morphology and phases present, different mechanisms apply for photocatalytic reactions. Xie and Yuan [55] studied the cerium ion (Ce^{4+}) modified TiO_2 sol and nanocrystallites, which were prepared by chemical hydrothermal synthesis methods. Figure 7 illustrates the photosensitized photocatalysis mechanism of dye in the Ce^{4+}-TiO_2 sol system. In this reaction mechanism, an excited electron from dye due to visible light transfers to Ce ion. The hole left on dye can extract electrons to form hydroxyl radicals ($HO^{\cdot}$). In this process, the electrons are trapped by Ce^{4+} ions and are subsequently utilized for the formation of superoxide radicals [56]. The presence of Ce^{4+} on the surface of nanoparticle could develop the below reactions:

$Ce^{4+} + e^- \rightarrow Ce^{3+}$ and $Ce^{3+} + O_2 \rightarrow Ce^{4+} + {}^{\cdot}O_2$

Photocatalytic degradation of dyes through semiconductor materials follows a complex path. Many researchers presented dye sensitization and subsequent charge transfer as a major reaction mechanism. Verma et al. presented photocatalytic reaction mechanism for the presence of ceria at the interface of anatase and rutile. Dependence of the catalyst's architecture and Ce content was explored by Verma et al. [57]. The unique architecture of Ce-TiO_2 system was synthesized via simple sol-gel method with varying Ce content. Doping of Ce inhibited transformation of anatase to stable rutile phase. As it was mentioned earlier that anatase has better photocatalytic activity, Ce doping showed a positive effect on photocatalytic activity which was measured by degradation of MB. Novel architecture material showed enhanced activity under a combination of ultraviolet and visible light. Reason for higher photocatalytic activity was sought to be the presence of CeO_2 at the interface of anatase and rutile, which thus facilitates excellent interfacial charge transfer as shown in Figure 8. In such systems, excitation of electron from valence band to conduction band of CeO_2 occur due to photoactivation via visible light ($E_g = 2.94$). However, CB electron of CeO_2 is not capable of reduction of O_2 due to its unfavorable redox potential position. This electron can transfer to CB of anatase and subsequently to rutile via interfacial charge transfer. An electron in CB of rutile can thermodynamically have accepted by O_2 adsorbed on the surface and create highly reactive superoxide anions by reduction reaction. On the contrary, holes can migrate to VB of CeO_2 to accept electron from adsorbed water and create ${}^{\cdot}OH^-$ (hydroxyl cation) [57].

Reaction mechanism can be summarized as follows:

(1) Photoactivation: Ce-TiO_2 (system) + hv ➔ $e^- + h^+$

(2) Ce^{4+} ➔ $Ce^{3+} + e^-$

(3) Interfacial charge transfer: e^-(CB Ce) ➔ e^-(CB anatase) ➔ e^-(CB rutile)

(4) Reduction: $O_2 + e^-$(CB rutile) ➔ ${}^{\cdot}O_2^-$

(5) ${}^{\cdot}O_2^-$ + organic dye ➔ degradation of dye

(6) Interfacial charge transfer: h^+ (VB rutile) ➔ h^+ (VB anatase) ➔ h^+ (VB Ce)

(7) Oxidation: h^+ (VB Ce) + H_2O ➔ $HO^{\cdot} + H^+$

(8) $HO^{\cdot}$ + Organic dye ➔ degradation of dye

1.7. Photocatalytic Activity Assessment by Methyl Blue Degradation. Some studies suggest that the hydroxyl radicals play a key role as reactants for oxidation of organic substrates in aqueous photocatalysis. Therefore, hydroxyl radicals yield is essential to determine the photocatalytic efficiency and for comparison of different photocatalytic materials. In order to assess the photocatalytic efficiency of a TiO_2-based catalyst, an organic and inorganic pollutant can be used as the environment. They can be divided into three categories: azo dyes [58], organic compounds [59], and inorganic gases [60]. Dye degradation is a popular method for assessing the efficiency because of its being fast and easy. Dyes have relatively high extinction coefficients to activate the photocatalyst, and they consequently will absorb a significant amount of the incoming light, which makes it difficult to assess the full photocatalytic activity [61].

Methylene blue (MB) is most commonly used as a model dye for the adsorption of organic dyes from aqueous solution [62]. It is a heterocyclic aromatic hydrocarbon with a molecular formula, $C_{16}H_{18}N_3SCl$ [63] (molecular weight 319.85 g/mol, maximum absorption wavelength 640). Methylene blue dye is commonly used in the textile, food, and chemical industries [64, 65]. As it is a commonly used dye in numerous industrial sectors, it can mix up with domestic water and pollute it. Therefore, it is crucial to remove this toxic dye from contaminated water by converting it to inorganic benign compounds by adding photocatalyst materials to wastewater [66, 67].

$C_{16}H_{18}N_3SCl + 25.5O_2$ ➔ $16CO_2 + 6H_2O + 3HNO_3 + H_2SO_4 + HCl$ [68, 69].

Methylene blue is found to give several environmental and health damages through contamination of water. Toxicity rate of MB is four and acute exposure by intravenous injection causes sweating, dizziness, confusion, vomiting, chest pain, and nausea [70].

The structures of the dye molecules directly decide the absorption characteristic of dyes for light. In the electron absorption spectra of dyes, there are several absorption bands, which reflect the state of motion of the electrons. The absorption wavelength, absorption intensity, and the

Table 3: Literature review on various preparation methods with process parameters of Ce-TiO_2 catalyst.

Materials	Dopant	Dopant concentration	Morphology	Bandgap, eV	Rate of degradation of MB dye (10^{-3} min^{-1})	References
TiO_2	Ce	3 mol	Nanoparticle	2.46	24	[72]
	Fe/Ce		Nanoparticle 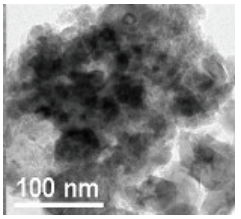	2.5	15.4	[74]
	Ce	1 wt %	Nanofiber 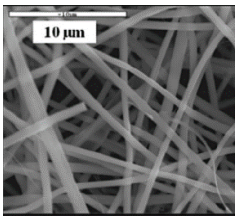	2.99	15	[75]
	Nd	1 wt %	Nanofiber 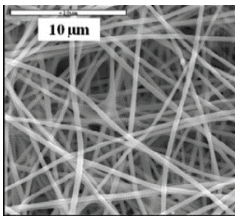	3.1	13	[75]
	Ce	5 wt %mol	Nanoparticle 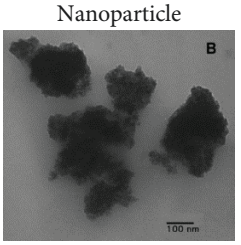		16.6	[76]
	Ce/N	0.6 mol	Nanoparticle	2.52		[77]
	Ce		Nanofibrous mats 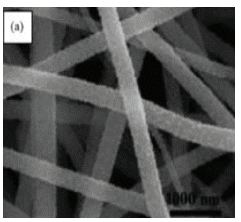		49.5	[53]
	Ce	5 mol %	Microsphere 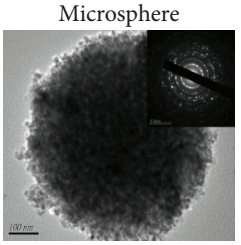	2.49	1.6	[71]

Table 3: Continued.

Materials	Dopant	Dopant concentration	Morphology	Bandgap, eV	Rate of degradation of MB dye (10^{-3} min^{-1})	References
	Ce/Pt	6.6 wt %	Nanoparticle 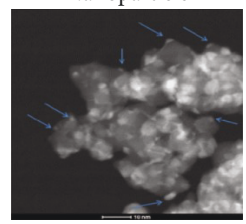	2.3		[78]
	Ce		Thin film	2.6	2.5	[79]
	Ce	2 mol	Nanobelt 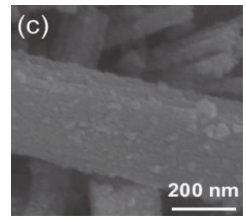	2.51	34.8	[80]
Degussa P25				3.2	6.3	

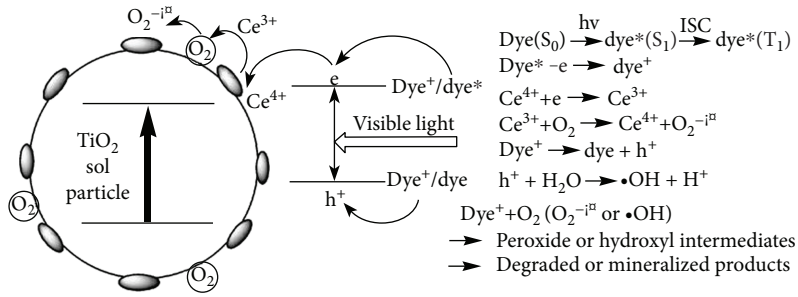

Figure 7: Photosensitized photocatalysis of Ce4+-TiO2 sol system (reprinted with permission from Xie and Yuan) [55].

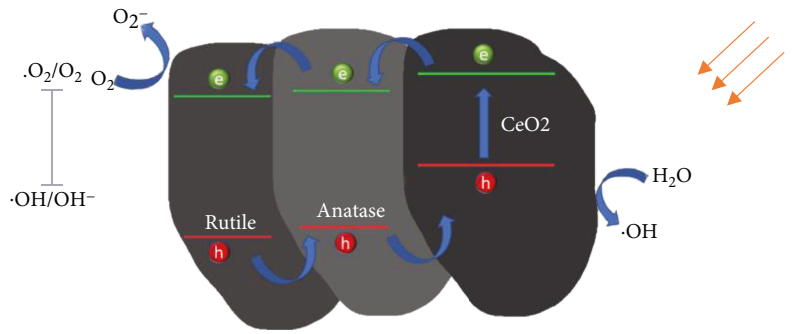

Figure 8: Interfacial charge transfer mechanism (adopted with permission from Verma et al.) [57].

shape of the absorption band are related directly to the structure of dye molecules. Therefore, it is possible to evaluate the structural variation of dyes by investigating the variation of the electron absorption spectra during the process of degradation of the dyes.

It has been reported that the photodecomposition of RhB aqueous solution in the presence of TiO_2 particles as a photocatalyst has two pathways: (1) the photocatalytic pathway which would occur under UV irradiation. In this pathway, TiO_2 would be activated to generate electrons under UV

irradiation ($\lambda \leq 385$ nm) to drive the process of photodegradation; (2) the photosensitization pathway which usually occurs under visible light irradiation. The bandgap of anatase TiO_2 is 3.2 eV; therefore, the energy of visible light ($\lambda > 400$ nm) is not enough to excite TiO_2 to produce electrons to drive the process of photodegradation. In the photosensitization pathway, where TiO_2 cannot be activated by visible light, dyes will absorb visible light irradiation and can be excited, which will drive the process of photodegradation. However, the existence of TiO_2 photocatalyst is a prerequisite and a crucial requirement to ensure electron carriers to contact with electron acceptors adsorbed on the TiO_2 surface, which will help in the process of photodecomposition.

Xie et al. [71] showed that doping content of Ce microspheres improved photocatalytic activity on the degradation of MB under visible light irradiation. Priyanka et al. [72] studied the photocatalytic activity of TiO_2 and Ce-doped TiO_2 nanoparticles in solar light, and the degradation of MB was monitored. Within 10 min of sunlight irradiation, the 3 mol % Ce-doped TiO_2 sample could degrade about 90% of MB dye and then the degradation was almost complete in 30 min.

2. Conclusion

TiO_2 being extensively used as a photocatalyst for degradation of organic dyes, modification of it by Ce doping for visible light activation has been presented in this review. Various synthesis processes along with different morphologies of Ce-doped TiO_2 are also summarized. Complex reaction mechanisms involved with Ce-doped TiO_2 with important aspects were discussed. Even though the above-mentioned reaction mechanisms occurred simultaneously, it is very difficult to conclude which mechanism is more dominating during photocatalytic degradation of dye. It would be a mere oversimplification of complex reaction mechanism to present with any one of above-mentioned reaction mechanism alone. Photocatalytic reaction mechanisms for brookite and complex systems require more elaboration. When contributions from surface area, bandgap, presence of phases, concentration of Ce, and morphology of nanomaterial are included, the complex yet complete reaction mechanism of Ce-doped TiO_2 system can be modeled. Such reaction mechanism provides the ground basis for designing better material for utilization of visible light for novel applications of visible light active photocatalysts. It is expected that this review will provide a fundamental understanding of remedies to overcome bare TiO_2 limitations.

Conflicts of Interest

The authors declare that they have no conflicts of interest.

Acknowledgments

This work has been supported by the National Science Foundation (NSF) CMMI 1724342.

References

[1] J. Lee and P. Gouma, *Sol-Gel Processed Oxide Photocatalysts. Sol-Gel Processing for Conventional and Alternative Energy*, Springer, 2012.

[2] M. H. Fulekar, B. Pathak, and R. K. Kale, *Environment and Sustainable Development*, M. Envi Fulekar, B. Pathak, and R. Kale, Eds., Springer, New Delhi, 2014.

[3] J. A. Byrne, B. R. Eggins, N. M. D. Brown, B. McKinney, and M. Rouse, "Immobilisation of TiO_2 powder for the treatment of polluted water," *Applied Catalysis B: Environmental*, vol. 17, no. 1-2, pp. 25–36, 1998.

[4] X. Chen and S. S. Mao, "Titanium dioxide nanomaterials: synthesis, properties, modifications, and applications," *Chemical Reviews*, vol. 107, no. 7, pp. 2891–2959, 2007.

[5] H. Yu, H. Irie, and K. Hashimoto, "Conduction band energy level control of titanium dioxide: toward an efficient visible-light-sensitive photocatalyst," *Journal of the American Chemical Society*, vol. 132, no. 20, pp. 6898-6899, 2010.

[6] A. Fujishima and K. Honda, "Electrochemical photolysis of water at a semiconductor electrode," *Nature*, vol. 238, no. 5358, pp. 37-38, 1972.

[7] Y. Nosaka and A. Y. Nosaka, "Generation and detection of reactive oxygen species in photocatalysis," *Chemical Reviews*, vol. 117, no. 17, pp. 11302–11336, 2017.

[8] A. L. Linsebigler, G. Lu, and J. T. Yates Jr, "Photocatalysis on TiO2 surfaces: principles, mechanisms, and selected results," *Chemical Reviews*, vol. 95, no. 3, pp. 735–758, 1995.

[9] C. Karunakaran and S. Senthilvelan, "Photooxidation of aniline on alumina with sunlight and artificial UV light," *Catalysis Communications*, vol. 6, no. 2, pp. 159–165, 2005.

[10] K. Kogo, H. Yoneyama, and H. Tamura, "Photocatalytic oxidation of cyanide on platinized titanium dioxide," *The Journal of Physical Chemistry*, vol. 84, no. 13, pp. 1705–1710, 1980.

[11] H. Ding, H. Sun, and Y. Shan, "Preparation and characterization of mesoporous SBA-15 supported dye-sensitized TiO_2 photocatalyst," *Journal of Photochemistry and Photobiology A: Chemistry*, vol. 169, no. 1, pp. 101–107, 2005.

[12] Y. Gao and H. Liu, "Preparation and catalytic property study of a novel kind of suspended photocatalyst of TiO_2-activated carbon immobilized on silicone rubber film," *Materials Chemistry and Physics*, vol. 92, no. 2-3, pp. 604–608, 2005.

[13] M. M. Haque and M. Muneer, "Photodegradation of norfloxacin in aqueous suspensions of titanium dioxide," *Journal of Hazardous Materials*, vol. 145, no. 1-2, pp. 51–57, 2007.

[14] J. Krýsa, M. Keppert, Jaromír Jirkovský, V. Štengl, and J. Šubrt, "The effect of thermal treatment on the properties of TiO_2 photocatalyst," *Materials Chemistry and Physics*, vol. 86, no. 2-3, pp. 333–339, 2004.

[15] H. Chun, W. Yizhong, and T. Hongxiao, "Destruction of phenol aqueous solution by photocatalysis or direct photolysis," *Chemosphere*, vol. 41, no. 8, pp. 1205–1209, 2000.

[16] R. Asahi, T. Morikawa, T. Ohwaki, K. Aoki, and Y. Taga, "Visible-light photocatalysis in nitrogen-doped titanium oxides," *Science*, vol. 293, no. 5528, pp. 269–271, 2001.

[17] D. Dambournet, I. Belharouak, and K. Amine, "Tailored preparation methods of TiO_2 anatase, rutile, brookite: mechanism of formation and electrochemical properties," *Chemistry of Materials*, vol. 22, no. 3, pp. 1173–1179, 2010.

[18] C. Suresh, V. Biju, P. Mukundan, and K. G. K. Warrier, "Anatase to rutile transformation in sol-gel titania by modification of precursor," *Polyhedron*, vol. 17, no. 18, pp. 3131–3135, 1998.

[19] K.-R. Zhu, M.-S. Zhang, J.-M. Hong, and Z. Yin, "Size effect on phase transition sequence of TiO_2 nanocrystal," *Materials Science and Engineering: A*, vol. 403, no. 1-2, pp. 87–93, 2005.

[20] A. Beltran, L. Gracia, and J. Andres, "Density functional theory study of the brookite surfaces and phase transitions between natural titania polymorphs," *The Journal of Physical Chemistry B*, vol. 110, no. 46, pp. 23417–23423, 2006.

[21] H. Zhang and J. F. Banfield, "Understanding polymorphic phase transformation behavior during growth of nanocrystalline aggregates: insights from TiO_2," *The Journal of Physical Chemistry B*, vol. 104, no. 15, pp. 3481–3487, 2000.

[22] P. I. Gouma, "Nanostructured polymorphic oxides for advanced chemosensors," *Reviews on Advanced Materials Science*, vol. 5, no. 147, p. 154, 2003.

[23] M. A. Fox and M. T. Dulay, "Heterogeneous photocatalysis," *Chemical Reviews*, vol. 93, no. 1, pp. 341–357, 1993.

[24] Y.-H. Tseng, C. S. Kuo, C. H. Huang et al., "Visible-light-responsive nano-TiO_2 with mixed crystal lattice and its photocatalytic activity," *Nanotechnology*, vol. 17, no. 10, pp. 2490–2497, 2006.

[25] Q. Tay, X. Liu, Y. Tang, Z. Jiang, T. C. Sum, and Z. Chen, "Enhanced photocatalytic hydrogen production with synergistic two-phase anatase/brookite TiO_2 nanostructures," *The Journal of Physical Chemistry C*, vol. 117, no. 29, pp. 14973–14982, 2013.

[26] K. Hashimoto, H. Irie, and A. Fujishima, "TiO_2 photocatalysis: a historical overview and future prospects," *Japanese Journal of Applied Physics*, vol. 44, no. 12, pp. 8269–8285, 2005.

[27] V. Subramanian, E. E. Wolf, and P. V. Kamat, "Catalysis with TiO_2/gold nanocomposites. Effect of metal particle size on the Fermi level equilibration," *Journal of the American Chemical Society*, vol. 126, no. 15, pp. 4943–4950, 2004.

[28] E. Bae and W. Choi, "Highly enhanced photoreductive degradation of perchlorinated compounds on dye-sensitized metal/TiO_2 under visible light," *Environmental Science & Technology*, vol. 37, no. 1, pp. 147–152, 2003.

[29] X. Chen, L. Liu, P. Y. Yu, and S. S. Mao, "Increasing solar absorption for photocatalysis with black hydrogenated titanium dioxide nanocrystals," *Science*, vol. 331, no. 6018, pp. 746–750, 2011.

[30] S. In, A. Orlov, R. Berg et al., "Effective visible light-activated B-doped and B,N-codoped TiO_2 photocatalysts," *Journal of the American Chemical Society*, vol. 129, no. 45, pp. 13790-13791, 2007.

[31] A. Kubacka, M. Fernández-García, and G. Colón, "Nanostructured Ti–M mixed-metal oxides: toward a visible light-driven photocatalyst," *Journal of Catalysis*, vol. 254, no. 2, pp. 272–284, 2008.

[32] G. Li, D. Zhang, and J. C. Yu, "Thermally stable ordered mesoporous CeO_2/TiO_2 visible-light photocatalysts," *Physical Chemistry Chemical Physics*, vol. 11, no. 19, pp. 3775–3782, 2009.

[33] W. Choi, A. Termin, and M. R. Hoffmann, "The role of metal ion dopants in quantum-sized TiO_2: correlation between photoreactivity and charge carrier recombination dynamics," *The Journal of Physical Chemistry*, vol. 98, no. 51, pp. 13669–13679, 1994.

[34] J.-C. G. Bünzli and C. Piguet, "Taking advantage of luminescent lanthanide ions," *Chemical Society Reviews*, vol. 34, no. 12, pp. 1048–1077, 2005.

[35] A.-W. Xu, Y. Gao, and H.-Q. Liu, "The preparation, characterization, and their photocatalytic activities of rare-earth-doped TiO_2 nanoparticles," *Journal of Catalysis*, vol. 207, no. 2, pp. 151–157, 2002.

[36] Y. Wang, H. Cheng, Y. Hao, J. Ma, W. Li, and S. Cai, "Photoelectrochemical properties of metal-ion-doped TiO_2 nanocrystalline electrodes," *Thin Solid Films*, vol. 349, no. 1-2, pp. 120–125, 1999.

[37] Y. Wang, H. Cheng, Y. Hao et al., "The photoelectrochemistry of Nd^3+-doped TiO_2 nanocrystalline electrodes," *Journal of Materials Science Letters*, vol. 18, no. 2, pp. 127–129, 1999.

[38] A. S. Ivanova, "Physicochemical and catalytic properties of systems based on CeO_2," *Kinetics and Catalysis*, vol. 50, no. 6, pp. 797–815, 2009.

[39] F. B. Li, X. Z. Li, M. F. Hou, K. W. Cheah, and W. C. H. Choy, "Enhanced photocatalytic activity of Ce^{3+}–TiO_2 for 2-mercaptobenzothiazole degradation in aqueous suspension for odour control," *Applied Catalysis A: General*, vol. 285, no. 1-2, pp. 181–189, 2005.

[40] T. Yu, X. Tan, L. Zhao, Y. Yin, P. Chen, and J. Wei, "Characterization, activity and kinetics of a visible light driven photocatalyst: cerium and nitrogen co-doped TiO_2 nanoparticles," *Chemical Engineering Journal*, vol. 157, no. 1, pp. 86–92, 2010.

[41] J. M. Coronado, A. Javier Maira, A. Martínez-Arias, J. C. Conesa, and J. Soria, "EPR study of the radicals formed upon UV irradiation of ceria-based photocatalysts," *Journal of Photochemistry and Photobiology A: Chemistry*, vol. 150, no. 1-3, pp. 213–221, 2002.

[42] Y. Zhang, A. H. Yuwono, J. Wang, and J. Li, "Enhanced photocatalysis by doping cerium into mesoporous titania thin films," *The Journal of Physical Chemistry C*, vol. 113, no. 51, pp. 21406–21412, 2009.

[43] J. Fang, H. Bao, B. He et al., "Interfacial and surface structures of CeO_2–TiO_2 mixed oxides," *The Journal of Physical Chemistry C*, vol. 111, no. 51, pp. 19078–19085, 2007.

[44] A. Trovarelli, *Catalysis by Ceria and Related Materials*, vol. 2, World Scientific, 2002.

[45] A. Tanaka, K. Hashimoto, and H. Kominami, "Photocatalytic mineralization of acetic acid in aqueous suspension of metal-loaded cerium (IV) oxide under irradiation of visible light," *Chemistry Letters*, vol. 40, no. 4, pp. 354–356, 2011.

[46] M. Sidheswaran and L. L. Tavlarides, "Characterization and visible light photocatalytic activity of cerium- and iron-doped titanium dioxide sol–gel materials," *Industrial & Engineering Chemistry Research*, vol. 48, no. 23, pp. 10292–10306, 2009.

[47] B. Grzmil, M. Gleń, B. Kic, and K. Lubkowski, "Preparation and characterization of single-modified TiO_2 for pigmentary applications," *Industrial & Engineering Chemistry Research*, vol. 50, no. 11, pp. 6535–6542, 2011.

[48] Z. Liu, B. Guo, L. Hong, and H. Jiang, "Preparation and characterization of cerium oxide doped TiO_2 nanoparticles," *Journal of Physics and Chemistry of Solids*, vol. 66, no. 1, pp. 161–167, 2005.

[49] J. Fang, X. Bi, D. Si, Z. Jiang, and W. Huang, "Spectroscopic studies of interfacial structures of CeO_2–TiO_2 mixed oxides," *Applied Surface Science*, vol. 253, no. 22, pp. 8952–8961, 2007.

[50] T. López, F. Rojas, R. Alexander-Katz, F. Galindo, A. Balankin, and A. Buljan, "Porosity, structural and fractal study of sol–gel TiO_2–CeO_2 mixed oxides," *Journal of Solid State Chemistry*, vol. 177, no. 6, pp. 1873–1885, 2004.

[51] X. Cao, X. Yang, H. Li, W. Huang, and X. Liu, "Investigation of Ce-TiO_2 photocatalyst and its application in asphalt- based specimens for NO degradation," *Construction and Building Materials*, vol. 148, pp. 824–832, 2017.

[52] M. Reli, N. Ambrožová, M. Šihor et al., "Novel cerium doped titania catalysts for photocatalytic decomposition of ammonia," *Applied Catalysis B: Environmental*, vol. 178, pp. 108–116, 2015.

[53] T. Cao, Y. Li, C. Wang, L. Wei, C. Shao, and Y. Liu, "Fabrication, structure, and enhanced photocatalytic properties of hierarchical CeO_2 nanostructures/TiO_2 nanofibers heterostructures," *Materials Research Bulletin*, vol. 45, no. 10, pp. 1406–1412, 2010.

[54] H. Eskandarloo, A. Badiei, and M. A. Behnajady, "TiO_2/CeO_2 hybrid photocatalyst with enhanced photocatalytic activity: optimization of synthesis variables," *Industrial & Engineering Chemistry Research*, vol. 53, no. 19, pp. 7847–7855, 2014.

[55] Y. Xie and C. Yuan, "Visible-light responsive cerium ion modified titania sol and nanocrystallites for X-3B dye photodegradation," *Applied Catalysis B: Environmental*, vol. 46, no. 2, pp. 251–259, 2003.

[56] J. Fonseca de Lima, M. H. Harunsani, D. J. Martin et al., "Control of chemical state of cerium in doped anatase TiO_2 by solvothermal synthesis and its application in photocatalytic water reduction," *Journal of Materials Chemistry A*, vol. 3, no. 18, pp. 9890–9898, 2015.

[57] R. Verma, S. K. Samdarshi, and J. Singh, "Hexagonal ceria located at the interface of anatase/rutile TiO_2 superstructure optimized for high activity under combined UV and visible-light irradiation," *The Journal of Physical Chemistry C*, vol. 119, no. 42, pp. 23899–23909, 2015.

[58] J. Tschirch, D. Bahnemann, M. Wark, and J. Rathouský, "A comparative study into the photocatalytic properties of thin mesoporous layers of TiO_2 with controlled mesoporosity," *Journal of Photochemistry and Photobiology A: Chemistry*, vol. 194, no. 2-3, pp. 181–188, 2008.

[59] D. M. Tobaldi, A. Tucci, G. Camera-Roda, G. Baldi, and L. Esposito, "Photocatalytic activity for exposed building materials," *Journal of the European Ceramic Society*, vol. 28, no. 14, pp. 2645–2652, 2008.

[60] M.-C. Lu, G.-D. Roam, J.-N. Chen, and C.-P. Huang, "Adsorption characteristics of dichlorvos onto hydrous titanium dioxide surface," *Water Research*, vol. 30, no. 7, pp. 1670–1676, 1996.

[61] Y. Cheng, H. Sun, W. Jin, and N. Xu, "Photocatalytic degradation of 4-chlorophenol with combustion synthesized TiO_2 under visible light irradiation," *Chemical Engineering Journal*, vol. 128, no. 2-3, pp. 127–133, 2007.

[62] S. Chandrasekhar and P. N. Pramada, "Rice husk ash as an adsorbent for methylene blue—effect of ashing temperature," *Adsorption*, vol. 12, no. 1, pp. 27–43, 2006.

[63] L. V. Jian-xiao, C. Ying, X. Guo-hong, Z. Ling-yun, and W. Su-fen, "Decoloration of methylene blue simulated wastewater using a UV-H_2O_2 combined system," *Journal of Water Reuse and Desalination*, vol. 1, no. 1, pp. 45–51, 2011.

[64] P. K. Gillman, "Methylene blue implicated in potentially fatal serotonin toxicity," *Anaesthesia*, vol. 61, no. 10, pp. 1013-1014, 2006.

[65] P. K. Gillman, B. K. W. Ng, A. J. D. Cameron, and R. W. Y. Liang, "Methylene blue is a potent monoamine oxidase inhibitor," *Canadian Journal of Anesthesia/Journal canadien d'anesthésie*, vol. 55, no. 5, pp. 311-312, 2008.

[66] A. Houas, H. Lachheb, M. Ksibi, E. Elaloui, C. Guillard, and J.-M. Herrmann, "Photocatalytic degradation pathway of methylene blue in water," *Applied Catalysis B: Environmental*, vol. 31, no. 2, pp. 145–157, 2001.

[67] Y.-J. Lin, S. L. Tseng, W. J. Huang, and W. J. Wu, "Enhanced photocatalysis of pentachlorophenol by metal-modified titanium (IV) oxide," *Journal of Environmental Science and Health, Part B*, vol. 41, no. 7, pp. 1143–1158, 2006.

[68] A. Mills, C. Hill, and P. K. J. Robertson, "Overview of the current ISO tests for photocatalytic materials," *Journal of Photochemistry and Photobiology A: Chemistry*, vol. 237, pp. 7–23, 2012.

[69] I. A. Salem and M. S. El-Maazawi, "Kinetics and mechanism of color removal of methylene blue with hydrogen peroxide catalyzed by some supported alumina surfaces," *Chemosphere*, vol. 41, no. 8, pp. 1173–1180, 2000.

[70] R. E. Gosselin, R. P. Smith, and H. C. Hodge, *Clinical Toxicology of Commercial Products*, Williams & Wilkins, 1984.

[71] J. Xie, D. Jiang, M. Chen et al., "Preparation and characterization of monodisperse Ce-doped TiO_2 microspheres with visible light photocatalytic activity," *Colloids and Surfaces A: Physicochemical and Engineering Aspects*, vol. 372, no. 1-3, pp. 107–114, 2010.

[72] K. P. Priyanka, S. Anu Tresa, O. P. Jaseentha, and T. Varghese, "Cerium doped nanotitania—extended spectral response for enhanced photocatalysis," *Materials Research Express*, vol. 1, no. 1, article 015003, 2014.

[73] X. Ye, J. Sha, Z. Jiao, and L. Zhang, "Thermoanalytical characteristic of nanocrystalline brookite-based titanium dioxide," *Nanostructured Materials*, vol. 8, no. 7, pp. 919–927, 1997.

[74] K. B. Jaimy, V. P. Safeena, S. Ghosh, N. Y. Hebalkar, and K. G. K. Warrier, "Photocatalytic activity enhancement in doped titanium dioxide by crystal defects," *Dalton Transactions*, vol. 41, no. 16, pp. 4824–4832, 2012.

[75] M. S. Hassan, T. Amna, O.-B. Yang, H.-C. Kim, and M.-S. Khil, "TiO_2 nanofibers doped with rare earth elements and their photocatalytic activity," *Ceramics International*, vol. 38, no. 7, pp. 5925–5930, 2012.

[76] N. Aman, P. K. Satapathy, T. Mishra, M. Mahato, and N. N. Das, "Synthesis and photocatalytic activity of mesoporous cerium doped TiO_2 as visible light sensitive photocatalyst," *Materials Research Bulletin*, vol. 47, no. 2, pp. 179–183, 2012.

[77] X. Sun, H. Liu, J. Dong, J. Wei, and Y. Zhang, "Preparation and characterization of Ce/N-Codoped TiO_2 particles for production of H2 by photocatalytic splitting water under visible light," *Catalysis Letters*, vol. 135, no. 3-4, pp. 219–225, 2010.

[78] S. Kundu, J. Ciston, S. D. Senanayake et al., "Exploring the structural and electronic properties of Pt/ceria-modified TiO_2 and its photocatalytic activity for water splitting under visible light," *The Journal of Physical Chemistry C*, vol. 116, no. 26, pp. 14062–14070, 2012.

[79] B. Liu, X. Zhao, N. Zhang, Q. Zhao, X. He, and J. Feng, "Photocatalytic mechanism of TiO_2–CeO_2 films prepared by magnetron sputtering under UV and visible light," *Surface Science*, vol. 595, no. 1-3, pp. 203–211, 2005.

[80] J. Tian, Y. Sang, Z. Zhao et al., "Enhanced photocatalytic performances of CeO_2/TiO_2 nanobelt heterostructures," *Small*, vol. 9, no. 22, pp. 3864–3872, 2013.

[81] Y. Zhang, M. K. Ram, E. K. Stefanakos, and D. Y. Goswami, "Synthesis, characterization, and applications of ZnO nanowires," *Journal of Nanomaterials*, vol. 2012, Article ID 624520, 22 pages, 2012.

[82] Z. L. Wang and X. Feng, "Polyhedral shapes of CeO_2 nanoparticles," *The Journal of Physical Chemistry B*, vol. 107, no. 49, pp. 13563–13566, 2003.